Cell Migration at the Interface of a Dual Chemical-Mechanical Gradient

N. A. Hale,[†] Y. Yang,[‡] and P. Rajagopalan*[,†]

Department of Chemical Engineering, Virginia Polytechnic Institute and State University, Blacksburg, Virginia 24061, and Department of Chemical Engineering, Lehigh University, Bethlehem, Pennsylvania 18015

ABSTRACT Cell migration plays a critical role in numerous physiological processes, such as wound healing, response to inflammation, and cancer metastasis. In recent years, accumulating evidence indicates that cell movement is regulated not only by chemical signals but also by mechanical stimuli. In this study, the primary goal is to identify whether a chemical or mechanical stimulus plays the decisive role in directing cell migration. Measuring the motility of cells when they are presented with a combination of chemical and mechanical cues will provide insight into the complex physiological phenomena that guide and direct migration. A novel polyacrylamide hydrogel was designed with an interfacial region where the chemical and mechanical properties varied in opposing directions. One side of the interface was stiff (high Young's modulus) with a low protein concentration, whereas the other side of the interface was compliant (low Young's modulus) with a high protein concentration. The chemical gradient was created by varying the collagen (type I) concentration and the mechanical gradient was introduced by changing the extent of cross-linking in the polymer. The length of the interface with opposing chemical-mechanical profiles was found to be approximately 100 μm. Our results demonstrate that when Balb/c 3T3 fibroblasts were presented with a choice, they either migrated preferentially toward the high-collagen-compliant (low Young's modulus) side of the interfacial region or remained on the high-collagen region, suggesting a more dominant role for chemical stimuli in directing fibroblast locomotion.

KEYWORDS: chemotaxis • mechanotaxis • AFM • cell migration

INTRODUCTION

Cell migration plays a significant role in many physiological processes, including embryonic development, immune response, wound healing, angiogenesis, and in cancer metastasis. In embryogenesis, cellular migration is considered to be a crucial factor for the development of tissues and organs (1−3). During inflammation, neutrophils and other cells responsible for mounting an immune response are guided toward the affected tissues (4−6). As a result, the phagocytosis of invading pathogens and the removal of toxins occurs. Fibroblasts and vascular endothelial cells migrate toward nascent scar tissue and deposit extracellular matrix proteins at the wounded site (7−10). Because of the presence of cells and the deposition of proteins, the mechanical properties of scar tissues change over time, leading ultimately to healing and wound closure. The successful utilization of tissue engineered devices and biomaterials are reliant on the ability of cells to migrate, proliferate, and colonize surfaces (11−13). Therefore, obtaining a comprehensive view of the complex combinations of stimuli that direct cell migration is a critical component in the design of therapeutics and implants, in organogenesis, and in disease progression.

Cells can sense and probe their surrounding environment and migrate both in vitro and in vivo in response to external signals. A wide range of stimuli or cues have been implicated in the modulation and direction of cell locomotion. These stimuli can be chemical (14−19), mechanical (20−30), optical (31), electrical, or magnetic (2, 32) in nature. Among these stimuli, migratory patterns in response to chemical and mechanical cues have been widely studied and reported. During chemotaxis, cells are able to sense the presence of extracellular chemical signals and migrate in the direction of the chemical concentration gradient. Several studies have also demonstrated that cells migrate in response to physical properties of their underlying substrates such as substrate rigidity, mechanical stress and topographic features (20−30, 33, 34). Lo and co-workers have shown that fibroblast motility can be governed purely by substrate rigidity (22). Poly(acrylamide) (PAAM) hydrogels were designed to exhibit a soft versus rigid side. When fibroblasts were cultured on this substrate, they exhibited directed migration from the soft regions toward the rigid side of the hydrogel substrate; however, cellular migration in the opposite direction did not occur. Vascular smooth muscle cells cultured on a radial gradient compliant substrate preferentially adhered and accumulated on surfaces that exhibit higher rigidity (27). More recently, substrate elasticity has been shown to play a determining role in directing the lineage of stem cells (29, 30). The ability for cells to assemble into tissuelike structures has been observed on soft substrates (33). Cells were observed to aggregate and to form clusters on soft surfaces; however, on stiff materials, they tend to spread,

* To whom correspondence should be addressed. Tel: (540) 231-4851. Fax: (540) 231-5022. E-mail: padmar@vt.edu.
Received for review April 20, 2010 and accepted June 29, 2010
[†] Virginia Polytechnic Institute and State University.
[‡] Lehigh University.
DOI: 10.1021/am100346k

suggesting a prominent role for elasticity in the formation of tissues (33). Cell locomotion guided by substrate rigidity has been shown to prevail in 3D scaffolds as well. In recent studies, growth-arrested dermal fibroblasts accumulated preferentially on the stiff end of a 3D collagen scaffold (35, 36). The mechanisms that direct cellular migration are still unclear because this physiological process is guided by chemical, mechanical, and several other stimuli and signals. The locomotion of a cell is dependent on the presence of cell-adhesive ligands to promote integrin-ligand interactions, optimal substrate rigidity, and matrix deformations that occur when cells exert contractile forces (37). Measuring cellular motility based solely upon a chemical or mechanical stimulus is not entirely representative of cell motility in vivo.

The primary objective of this study is to monitor cell locomotion when cells are simultaneously presented with opposing chemical and mechanical cues. PAAM hydrogels were designed to exhibit a chemical−mechanical interface where the chemical and mechanical gradients were in opposing directions. PAAM hydrogels were chosen as the substrate for multiple reasons. First, their mechanical properties can be easily tuned over a wide range of elastic moduli simply by changing the cross-linker concentration (22, 26). Second, the surface of PAAM hydrogels is inert unless modified chemically. These hydrogels can be linked covalently to proteins and peptides to render them biocompatible. Third, they are optical transparent, enabling their use in optical microscopy (22, 26). A chemical gradient was introduced by varying type 1 collagen concentration and the mechanical gradient was introduced by changing the extent of cross-linking. Type 1 collagen was used to create the chemical gradient because collagen is found in the extracellular matrix (ECM). In this study, the migratory patterns of fibroblasts were monitored because fibroblasts are found in several tissues and organs and are also motile. Fibroblasts that were adhered within the interfacial region were presented with a choice in the direction of their locomotion. They could choose to move toward either the high collagen−low Young's modulus or low collagen−high Young's modulus sides of the interface. The migratory behavior of fibroblasts on three different interfacial regions was monitored to obtain insight into the roles played by chemical and mechanical signals.

MATERIALS AND METHODS

Materials. Glutaraldehyde (50% v/v solution, Electron Microscopy Sciences, Hatfield, PA), 3-triethoxysilylpropylamine (3-APTES, Sigma-Aldrich Chemical Co., St. Louis, MO), acrylamide solution (40% v/v solution, Bio-Rad, Hercules, CA), *N*,*N*,*N*′,*N*′-tetramethylethylenediamine (TEMED, 0.1 g/mL, Bio-Rad), bis-acrylamide solution (2% v/v solution, Bio-Rad), ammonium persulfate (AP, 0.1 g/mL, Bio-Rad), and phosphate-buffered saline (PBS, Invitrogen, Carlsbad CA) were used as received.

Methods. ***Activation of Glass Coverslips.*** Glass coverslips (25 mm in diameter, Fisher Scientific, Pittsburgh, PA) were activated to ensure a durable bond between the polyacrylamide (PAAM) hydrogel and the glass surface (38). These coverslips were passed briefly through an oxidizing flame to remove hydrocarbon residues. The coverslips were cooled and then coated with a thin layer of 0.1N NaOH solution and air-dried. Upon drying, a thin layer of 3-APTES was coated on the coverslips. The coverslips were immersed in a 8% v/v (diluted in 1X PBS) glutaraldehyde solution overnight, subsequently rinsed several times in deionized (DI) water, and stored at 4 °C until used.

Design of PAAM Hydrogels with a Gradient in Chemical and Mechanical Properties. PAAM hydrogels with a gradient in Young's modulus values were prepared in the following manner. Two monomer solutions were prepared with varying concentrations of the cross-linker. Each solution contained 0.8% v/v acrylamide. The concentration of the bis-acrylamide cross-linker was varied between 0.2 and 0.72% v/v in the monomer solutions. DI water was added to maintain the volume of both solutions at 10 mL. Fifteen microliters of TEMED and 50 μL of AP were added to both solutions. Red-fluorescent rhodamine beads (0.5% v/v, 0.5 μm Fluospheres, carboxylate-modified, rhodamine-conjugated microspheres, Invitrogen) were added only to the solution that contained a higher concentration of bis-acrylamide (0.56 or 0.72% v/v). Green-fluorescent type 1 collagen-conjugated FITC beads were added to both monomer solutions, however, the concentrations were varied. In the solution that contained a low concentration of bis-acrylamide, the concentration of the green-fluorescent type 1 collagen coated beads was approximately 10-fold higher in comparison to the monomer solution that contained a high cross-linker concentration. To obtain gels with opposing chemical and mechanical gradients, 10 μL droplets of each monomer solution were placed next to each other on an activated glass coverslip (25 mm diameter) (22). In order to ensure a flat hydrogel surface, an 18 mm diameter cover slip was placed on top of the monomer droplet. Upon polymerization, PAAM hydrogels were obtained, where one side of the interface was highly cross-linked with a lower collagen concentration and the other side was lightly cross-linked with a higher collagen concentration. The gradient in mechanical properties was introduced by using two different monomer solutions (designated as monomer A and monomer B) that each contained different cross-linker concentrations. The three hydrogels synthesized were 0.2% v/v (monomer A)−0.72% v/v (monomer B), 0.2% v/v (monomer A)−0.56% v/v (monomer B), and 0.56% v/v (monomer A)−0.72% v/v (monomer B), indicating that each hydrogel was formed by monomer solutions that contain either 0.2, 0.56, or 0.72% v/v bis-acrylamide. After polymerization, the gels were rinsed overnight in cold DI water to remove any residual monomer and sterilized under a germicidal UV lamp for 1 h prior to cell culture. In subsequent sections, the hydrogels are identified by the bis-acrylamide content in the hydrogel, specifically, 0.2, 0.56, and 0.72% v/v.

The height of the PAAM hydrogel substrate was measured using fluorescence microscopy. Briefly, the distance between the upper and bottom layer of the beads was measured and this distance was estimated as the height of the gel.

Young's Modulus Measurements. The Young's modulus of PAAM hydrogels with and without fluorescent beads was determined by atomic force microscopy (AFM) measurements. AFM measurements were conducted on hydrated PAAM hydrogel samples on a Veeco Dimensions 3100 Nanoman AFM instrument. Measurements were conducted in contact mode using pyramidal-tipped silicon nitride cantilever (DNP-20) tips with a spring constant of 60 pN nm^{-1}. The tips were blunted with a half open angle of 36° to minimize penetration into the PAAM gel and force curves were obtained at 2 Hz. A Hertz-cone model was used to calculate the elastic modulus for tip deflections up to 2 μm (39, 40). The Young's modulus was calculated using a combination of Hooke's Law and the Hertz model (eqs 1 and 2, respectively).

$$F = \text{applied force} = k(d - d_0) \quad (1)$$

$$F = \frac{2\tan\alpha}{\pi}\left[\frac{E}{1-\nu^2}\right]\delta^2 \quad (2)$$

where F = applied force, $\alpha = 36°$, E = Young's modulus, k = spring constant of the cantilever, ν = Poisson's ratio (maintained at a constant value of 0.4), d = deflection of the cantilever, and δ = indentation. Measurements were initially conducted on homogeneous (single monomer) PAAM samples to determine mechanical properties of these hydrogels. Next, measurements were conducted on samples that were synthesized using two monomer solutions with different bis-acrylamide concentrations. AFM measurements were taken on either side of the chemical−mechanical interface in order to determine the change in mechanical properties that result as a function of the mixing of the two monomer solutions. Three sets of hydrogels were synthesized using monomers containing varying concentrations of bis-acrylamide. These hydrogels were 0.2% v/v (monomer A)−0.72% v/v (monomer B), 0.2% v/v (monomer A)−0.56% v/v (monomer B), and 0.56% v/v (monomer A)−0.72% v/v (monomer B), indicating that the hydrogel was formed by the polymerization of two drops of monomer solutions placed adjacent to each other. First, the interface was identified using an optical microscope and this position was designated as 0 μm. Indentations were made at the zero position (the interface) and at ±10, ±20, ±50, ±100, ±200, and ±1000 μm from the estimated center position. The positive and negative signs denote that measurements were taken on both sides of the interface. Measurements were also taken at three difference locations along the chemical−mechanical interface. To ensure that the gels remained hydrated during the time frame of the measurements, we added approximately 50 μL of 1X PBS to the gel every 5−10 min.

Surface Concentration of Type 1 Collagen-Coated Beads. FITC-type 1 collagen beads were added to both monomer solutions and the unit surface area occupied by these beads was expected to vary in the interfacial region. Fluorescence microscopy was used to calculate the unit area covered by the collagen-coated beads. The interface was identified by merging fluorescent images of the red-fluorescent rhodamine and the green-fluorescent FITC beads. Rectangular cross-sections of the sample were drawn on either side of the interface that extended well beyond the interfacial region. Only those beads that were in focus and present on the uppermost layer of the PAAM hydrogel were used to calculate the surface area occupied by the fluorescent beads in each rectangular cross-section. The surface areas occupied by beads that were out of focus or blurred were not included because they were presumed to be located in the subsurface regions of the hydrogel and therefore inaccessible to the cells. The area occupied by the FITC-collagen beads in each rectangular area was measured using Nikon Elements imaging software and normalized to the total area of the rectangle.

Cell Culture. Balb/c 3T3 cells (Balb/3T3 clone A31, American Type Culture Collection, Manassas, VA) were maintained at 37 °C and 5% CO_2 in Dulbecco's modified Eagle's medium (DMEM, Invitrogen) supplemented with 10% v/v bovine calf serum (Hyclone, Logan, UT) and 2% v/v penicillin-streptomycin (Invitrogen). Projected cell areas were measured using Nikon Elements (Ardmore, PA) software. The mean and standard deviation values were calculated for approximately 50 cells per condition.

Cell Migration Studies. For cell migration measurements, Balb/c 3T3 fibroblast cells were cultured on PAAM hydrogels at a low cell density (≈100 000 cells/cm^2). In these measurements, fibroblasts were maintained between passages 10−20 and experiments were conducted within 16 h of cell-seeding. The samples were placed on an optical microscope (Nikon, Eclipse, TE2000-U, Ardmore, PA). The microscope was equipped with 10, 20, and 40× objectives, a motorized stage, and an environmental chamber maintained at 37 °C and 5% CO_2. Phase-contrast images of the cell and fluorescent images of the rhodamine and collagen marker beads embedded in the substratum were analyzed using Nikon Elements imaging software. Phase-contrast images of fibroblasts and the fluorescent images of rhodamine or collagen-conjugated FITC beads were captured every 30 min up to 6 h using time-lapse microscopy. Only cells that fit the criteria listed below were included in the analysis. Cells that died, underwent mitosis, or collided with each other during the observation period were excluded. The "x" and "y" coordinates of the cell centroids were measured at each time point. The mean-squared displacement ($\langle d^2 \rangle$) was calculated and this value was used to measure cellular translocation and speed. For a cell tracked for a total time $t_{max} = N\Delta t$ with a series of real time coordinate $\{x(n\Delta t), y(n\Delta t)\}$

$$\langle d^2, t = n\Delta t\rangle = \frac{1}{(N-n+1)}\sum_{i=0}^{i=N-n}[(x(n+i)\Delta t - x(i\Delta t)]^2 + [y(n+i)\Delta t - y(i\Delta t)]^2 \quad (3)$$

Cell Migration in the Presence of Mitomycin C. The migration of growth-arrested fibroblasts was investigated over a five-day period. Fibroblast culture medium was supplemented with 10 μg/mL mitomycin C (Sigma-Aldrich) and added to the samples immediately after cell-seeding. Fibroblasts were exposed to the mitomycin-C containing culture medium for 2 h. The culture medium was removed and the cultures were maintained in standard fibroblast culture medium. Multiple positions along the interface on the PAAM samples were identified, and each location was imaged every 24 h over a 5-day period to monitor cell accumulation at specific locations along the interface.

Statistical Analysis. Statistical significance and p-values between sample groups were determined by t test analysis with alpha set to 0.05. All data are reported as mean ± standard deviation. Sample sizes are denoted by n.

The binomial test was performed to assess the statistical significance of the trends in cell migration. The null hypothesis was that cells would not show a preference to migrate toward the high-collagen region over the low-collagen side of the interface. The alternate hypothesis was that the cells would preferentially migrate to the high-collagen side of the interface. Hence, according to the null hypothesis, the probability that a cell would move toward a high-collagen-concentration area was 0.5. Suppose that out of a total of l cells, we observed k cells moving toward high collagen concentration. Then, under the null hypothesis, the probability that we would observe k or more out of l cells moving toward high collagen concentration is provided in eq 4. This quantity is the p-value of the binomial test. Alpha was maintained at a value of 0.05.

$$\sum_{i=k}^{l}\binom{l}{i}\left(\frac{1}{2}\right)^i\left(\frac{1}{2}\right)^{l-i} = \sum_{i=k}^{l}\binom{l}{i}\left(\frac{1}{2}\right)^l \quad (4)$$

RESULTS

Polyacrylamide (PAAM) hydrogels were designed with chemical and mechanical gradients in opposite directions. Fluorescent images of the PAAM hydrogel depict a 2D substrate with varying chemical and mechanical profiles (Figure 1A,B). Because of the mixing of the two monomer mixtures prior to the completion of polymerization, an interfacial region with chemical and mechanical gradients

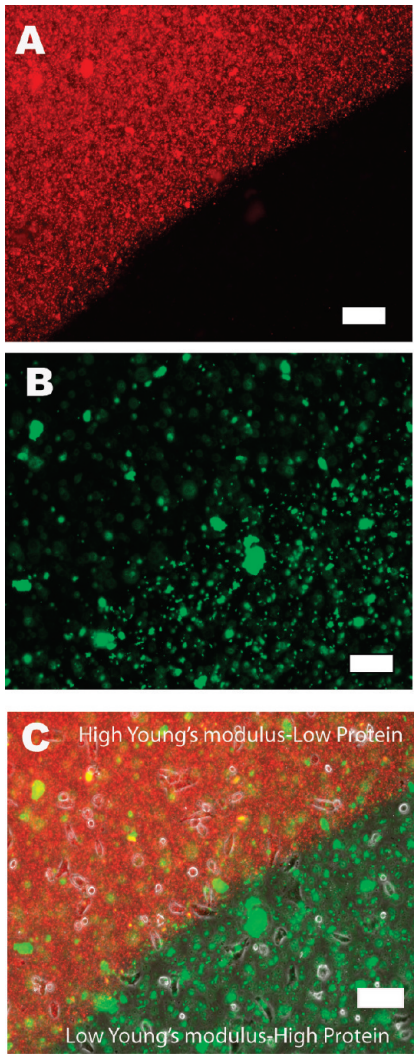

FIGURE 1. PAAM hydrogel derived from two monomer droplets. Fluorescent images of: (A) high Young's modulus region with rhodamine-conjugated polystyrene beads; (B) low Young's modulus region with type 1 collagen, FITC-conjugated polystyrene beads; (C) merged fluorescence and phase contrast images of the hydrogel substrate and adherent fibroblasts. Scale bar = 50 μm.

was created. In this region, the hydrogel was formed from both monomer solutions and contained both green and red fluorescent beads at varying concentrations. One side of the interfacial region contained primarily rhodamine-conjugated fluorescent beads and the other side exhibited primarily FITC-conjugated type 1 collagen beads. These two domains were defined as the two ends of the interfacial region with the center defined, for the purposes of this study, as the interface. Within the interfacial region, chemical and mechanical properties varied, and therefore this area was the focus of the cell migration studies. Balb/c 3T3 fibroblasts were cultured on the PAAM hydrogels and were found to adhere on both sides of the interface within 3 h of cell-seeding (Figure 1C). The height of the PAAM substrate was found to be approximately 100 μm and did not vary at and near the vicinity of the interface.

AFM measurements were conducted to determine changes in the mechanical properties in the interfacial region. These measurements were first conducted on homogeneous PAAM

Table 1. Young's Modulus Values for Homogeneous PAAM Gels Measured by Atomic Force Microscopy

bis-acrylamide concentration in PAAM hydrogels (% v/v)	beads	Young's modulus (kPa)	n
0.2	no	31.2 ± 2.1	3
0.56	no	52.7 ± 5.4	3
0.72	no	79.8 ± 6.5	3
0.2	yes	35.1 ± 4.3	3
0.56	yes	53.9 ± 2.4	3
0.72	yes	84.7 ± 1.7	3

hydrogels that were synthesized from a single monomer that contained a specific cross-linker concentration, in the absence and presence of fluorescent beads (Table 1). When fluorescent beads were not added to the reactant mixture, the Young's modulus of homogeneous PAAM hydrogels that contained either 0.2, 0.56, or, 0.72% v/v of the bis-acrylamide cross-linker was found to be 31.2 ± 2.1, 52.7 ± 5.4, and 79.8 ± 6.5 kPa, respectively. When fluorescent beads were incorporated into the hydrogels, the Young's modulus values at cross-linker concentrations of 0.2, 0.56, or, 0.72% v/v were found to be 35.1 ± 4.3, 53.9 ± 2.4, and 84.6 ± 1.7 kPa, respectively. The incorporation of the fluorescent beads did not result in significant increases to the Young's modulus values. For example, in gels that contained 0.2% v/v bis-acrylamide, the increase in modulus was approximately 10%. When the bis-acrylamide concentration was either 0.56 or 0.72% v/v, the increase in modulus was 2.2 and 5.6%, respectively.

Because the monomer solutions used to prepare the hydrogel mixed prior to polymerization, the mechanical properties at the interface were expected to vary from those determined for the homogeneous hydrogels. The gradient in mechanical properties was introduced by using two different monomer solutions (designated henceforth as monomer A and monomer B) that each contained different cross-linker concentrations. The three PAAM substrates used in this study were obtained from the mixing of two monomer droplets, namely, 0.2% v/v (monomer A)−0.56% v/v (monomer B), 0.2% v/v (monomer A)−0.72% v/v (monomer B), and 0.56% v/v (monomer A)−0.72% v/v (monomer B). AFM measurements were conducted at the interface and at fixed distances from the interface to determine the length scale through which the mechanical properties varied. Measurements were taken up to 1000 μm on either side of the chemical-mechanical interface for the three hydrogel interfaces. The distance through which varying Young's modulus values were observed was found to be 24 ± 11.4, 32 ± 13.03, and 12.5 ± 5 μm for the 0.2% v/v (monomer A)−0.56% v/v (monomer B), 0.2% v/v (monomer A)−0.72% v/v (monomer B), and 0.56% v/v (monomer A)−0.72% v/v (monomer B) hydrogel substrates respectively (Table 2). These results suggest that because of the mixing of the two monomer solutions, the mechanical properties differed from those obtained for homogeneous gels. The length of the mechanical gradient was observed to be relatively short, varying from approximately 10 to 45 μm. Beyond this

Table 2. Length of the Interfacial Region with Variations in Values of Young'S Modulus; Measurements Conducted Using Atomic Force Microscopy

PAAM hydrogels that exhibit an interfacial region	length of the interfacial region that exhibits a mechanical gradient (varying Young's modulus values) (μm)	n
0.2 % v/v (monomer A)−0.56 % v/v (monomer B)	24 ± 11.4	5
0.2 % v/v (monomer A)−0.72 % v/v (monomer B)	32 ± 13.03	5
0.56 % v/v (monomer A)−0.72 % v/v (monomer B)	12.5 ± 5	4

length-scale, the Young's modulus values were found to be identical to those obtained for homogeneous PAAM gels.

Because the concentration of the type 1 collagen beads was varied in the monomer solutions, the collagen concentration per unit area was expected to vary within the interfacial region. In the gradient hydrogels, the surface area occupied by the FITC- Type 1 collagen beads per unit area of the PAAM hydrogel was calculated up to 2000 μm on either side of the chemical−mechanical interface. A representative image of the collagen bead distribution on the interfacial region is shown in Figure 2. The average area occupied by collagen-coated FITC beads per unit area on the high- and low-collagen-concentration regions was measured at three different locations along the interface for each PAAM hydrogel. The area occupied by the collagen beads was found to vary within only approximately 50 μm on either side of the interface. Beyond this distance, the concentration of the FITC-collagen beads per unit area of the hydrogel surface was constant, indicating homogeneity in these regions. In the 0.2 % v/v (monomer A)−0.56 % v/v (monomer B) substrate, the fraction of the area occupied by the FITC type 1 collagen beads was found to be 263.3 ± 29 and 92 ± 28 μm^2 at the high-collagen and low-collagen sides of the interfacial region. In the 0.2 % v/v (monomer A)−0.72 % v/v (monomer B) PAAM surface, the area occupied by the collagen-coated beads ranged from 344.4 ± 46 μm^2 (high collagen) to 192.8 ± 57.5 μm^2 (low collagen) and in the 0.56 % v/v (monomer A)−0.72 % v/v (monomer B) hydrogel, these values were 245.7 ± 82.6 μm^2 (high collagen) and 96.7 ± 13.8 μm^2 (low collagen). On the basis of these data, the increase in the area occupied by the FITC-type 1 collagen bead concentration from the high modulus (low collagen concentration) to the low modulus (high collagen concentration) was found to be 2.8, 1.9, and 2.7 for the 0.2 % v/v (monomer A)−0.56 % v/v (monomer B), 0.2 % v/v (monomer A)−0.72 % v/v (monomer B), and 0.56 % v/v (monomer A)−0.72 % v/v (monomer B) hydrogels, respectively. On the basis of the AFM measurements and the collagen concentration results, the interfacial region spanned approximately 100 μm.

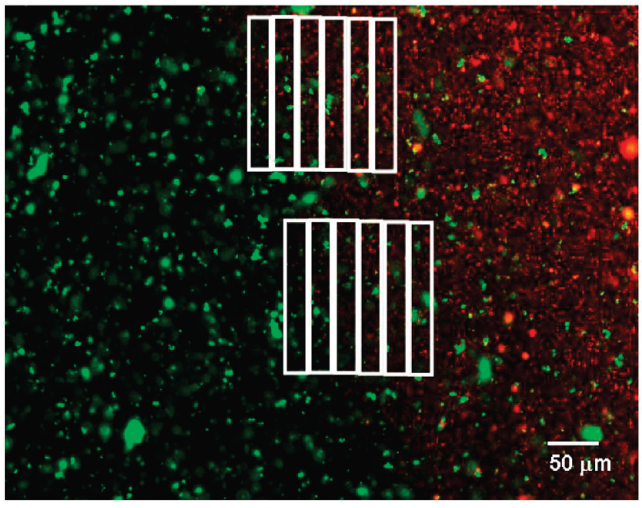

FIGURE 2. Representative image of an interfacial region with variations in collagen-FITC-polystyrene bead distribution. The rectangles denote regions in which the surface area of the beads were measured.

Projected cell areas were measured for cells adhered on the two sides of the interfacial region and the data are provided in Table 3. In all three interfacial regions, the projected cell areas were higher on the high collagen−low modulus side of the interface and these values were found to be statistically significant.

Because the primary purpose of this study was to obtain information on the effect of simultaneous chemical and mechanical stimuli on cell migration, measurements on cellular speed and direction of motion were focused upon cells located within the interfacial region. In general, the majority of cells migrated preferentially toward the high collagen−low modulus end of the interfacial region in all three PAAM substrates that were investigated. Among the cells that moved across the interfacial region approximately 87 % migrated toward the high collagen−low modulus interfacial region in the 0.2 % v/v (monomer A)−0.56 % v/v (monomer B) PAAM substrate (Table 4). The corresponding values in the 0.2 % v/v (monomer A)−0.72 % v/v (monomer B) and 0.56 % v/v (monomer A) −0.72 % v/v (monomer B) hydrogels were found to be 100 and 83 %, respectively.

Figure 3A−C depicts the time-lapse motion of a fibroblast on the low collagen−high Young's modulus side of the interface moving toward the high collagen−low Young's modulus end over a 3 h time period. The average velocity for fibroblasts moving from the low collagen−high Young's modulus side to the high collagen−low Young's modulus end of the interfacial region was found to be 11.01 ± 5.2, 9.64 ± 2.11, and 19.2 ± 9.7 μm/h in the 0.2 % v/v (monomer A)−0.56 % v/v (monomer B), 0.2 % v/v (monomer A)−0.72 % v/v (monomer B), and 0.56 % v/v (monomer A)−0.72 % v/v (monomer B) hydrogels, respectively. Among the three PAAM substrates investigated, fibroblasts cultured on the 0.56 % v/v (monomer A) −0.72 % v/v (monomer B) PAAM surface exhibited the highest average speed. The difference between the average migration speed for cells adherent on 0.2 % v/v (monomer A)−0.56 % v/v (monomer B) and on 0.2 % v/v (monomer A)−0.72 % v/v (monomer B) PAAM substrates was statistically insignificant (p-value of t test

Table 3. Projected Cell Areas for Cells on the High Collagen−Low Modulus and Low Collagen−High Modulus Regions of the Interface

PAAM hydrogels that exhibit an interfacial region	projected cell areas on high collagen−low modulus region (μm^2)	projected cell areas on high modulus−low collagen region (μm^2)	p-value
0.2% v/v (monomer A)−0.56% v/v (monomer B)	410.4 ± 292	280.9 ± 164.6	0.004
0.2% v/v (monomer A)−0.72% v/v (monomer B)	854.4 ± 349.9	394.3 ± 207.5	1.6×10^{-10}
0.56% v/v (monomer A)−0.72% v/v (monomer B)	1298.5 ± 505.6	496.8 ± 239.9	2.32×10^{-10}

Table 4. Summary of Results on the Directed Migration for Balb/c 3T3 Fibroblasts Adhered on the Interfacial Region

PAAM hydrogels that exhibit an interfacial region	motion toward high collagen−low young's modulus	motion toward low collagen−high young's modulus	cells that moved up or down along the high-collagen end of the interface	cells that moved up or down along the low-collagen end of the interface
0.2% v/v (monomer A)−0.56% v/v (monomer B)	13	2	10	2
0.2% v/v (monomer A)−0.72% v/v (monomer B)	5	0	6	4
0.56% v/v (monomer A)−0.72% v/v (monomer B)	10	2	6	1

>0.5). However, the difference in the average migration speed was found to be statistically significant between the 0.2% v/v (monomer A)−0.56% v/v (monomer B) and 0.56% v/v (monomer A)−0.72% v/v (monomer B) hydrogels (p-value=0.03) and between the 0.56% v/v (monomer A)−0.72% v/v (monomer B) and 0.2% v/v (monomer A)−0.72% v/v (monomer B) PAAM substrates (p-value =0.01).

There were several cells that did not choose to migrate across the interfacial region. In each of the three PAAM substrates, the percentage of cells that did not migrate across the chemical−mechanical interface ranged from 40−66%. The majority of cells that did not migrate across the interface, preferred to remain on the high collagen−low modulus end of the interface. These fibroblasts would explore the surrounding region by initially extending several lamellipodia and would subsequently retract them. They exhibited preferential motion either up or down the interface but did not cross the interfacial region. An example of such cellular behavior is shown in Figure 4. A fibroblast adhered on the interfacial region of a 0.2% v/v (monomer A)−0.72% v/v (monomer B) substrate, extended multiple lamellipodia in the first 2 h but did not exhibit motion toward the low collagen−high Young's modulus region. At the end of the third hour, the lamellipodia were withdrawn and the cell chose to remain on the high collagen−low Young's modulus side of the interface.

The average cell speed for fibroblasts that remained on the high collagen−low Young's modulus side of the interface, was found to be 16.4 ± 5.9, 8.8 ± 3.2, and 15.8 ± 3.8 μm/h in the 0.2% v/v (monomer A)−0.56% v/v (monomer B), 0.2% v/v (monomer A)−0.72% v/v (monomer B), and 0.56% v/v (monomer A)−0.72% v/v (monomer B) hydrogels, respectively. It is hypothesized that the lower values for cellular velocity exhibited by fibroblasts on the 0.2% v/v (monomer A)−0.72% v/v (monomer B) surface could be a result of the higher surface coverage by the type 1 collagen beads (8.5%) in comparison to the other substrates. Because cellular speed has been shown to have a biphasic relationship with chemical concentration (40), a higher collagen surface concentration may result in low velocity. The binomial test was performed to assess the statistical significance of the trends shown in Table 5. The columns titled "p-value" in Table 5 show the results of applying the binomial test to the cell migration trends. For all three substrates, the p-values of the tests comparing the number of cells that moved toward the high-collagen region to the number that moved toward the low-collagen region were significant at an alpha value of 0.05 (column 2, Table 5). The p-values were significant when we added the number of cells moving up

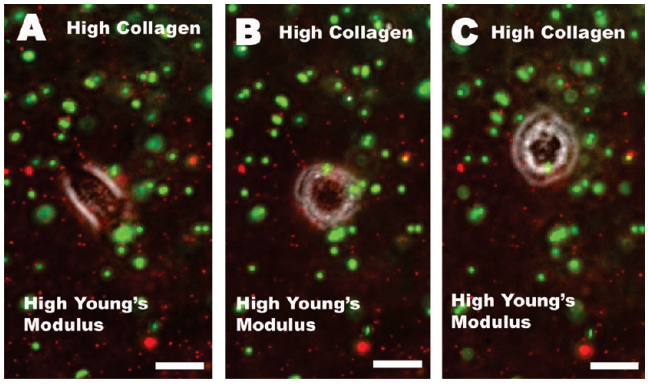

FIGURE 3. Time lapse images of fibroblast motion on a 0.2% v/v (monomer A)−0.56% v/v (monomer B) PAAM substrate. Cells migrated from the low collagen−high Young's modulus to high collagen−low Young's modulus side of the interfacial region. (A) t = 0, (B) t = 1 h, (C) t =3 h. Scale bar = 50 μm.

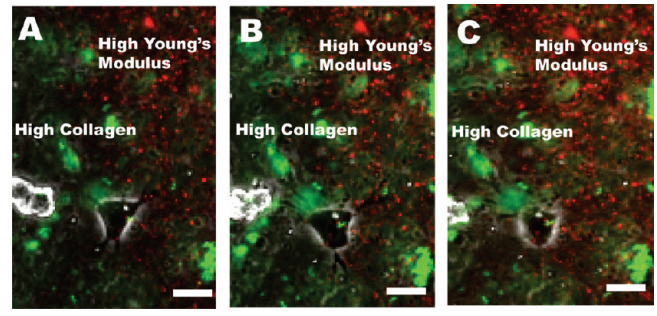

FIGURE 4. Time lapse images of a fibroblast on a 0.2% v/v (monomer A)−0.72% v/v (monomer B) PAAM substrate. The cell explores the low collagen−high Young's modulus region by extending lamellipodia but does not move across the interfacial region. (A) t = 0, (B) t = 1 h, (C) t = 3 h. Scale bar = 50 μm.

Table 5. *p*-Values Obtained from a Binomial Test That Was Conducted to Assess the Statistical Significance of the Trends in Cell Migration

PAAM hydrogels that exhibit an interfacial region	*p*-value for motion toward high-collagen region versus low collagen	p-value for motion (toward high collagen + along high-collagen region) versus (to low-collagen region + along low-collagen region)	*p*-value for motion to high-collagen region versus along high-collagen region
0.2 % v/v (monomer A)−0.56 % v/v (monomer B)	0.003	0.0002	0.34
0.2 % v/v (monomer A)−0.72 % v/v (monomer B)	0.01	0.002	0.73
0.56 % v/v (monomer A)−0.72 % v/v (monomer B)	0.03	0.06	0.23

and down each region (column 3, Table 5). These results suggest that cells showed a preference to migrate to or remain on the high collagen−low modulus side of the interfacial region. When we compared the number of cells moving toward the high-collagen region to the number of cells moving along the high-collagen region, none of the three *p*-values were significant (column 4, Table 5). The last set of *p*-values indicate that cells may not show a preference between migrating up and down the high-collagen region and moving toward the high-collagen region.

To determine if directed migration toward the high collagen−low modulus end of the interface prevailed over longer time periods, fibroblasts were growth-arrested with mitomycin C and imaged at different locations over a 5 day period. Figure 5 shows cellular aggregation at a specific location in the interfacial region for 0.2 % v/v (monomer A)−0.56 % v/v (monomer B) (Figure 5A,B), and 0.2 % v/v (monomer A)−0.72 % v/v (monomer B) (Figure 5C,D) PAAM hydrogels. On both substrates, cells accumulated on the high collagen−low modulus side of the interface. On the 0.2 % v/v (monomer A)−0.56 % v/v (monomer B) substrate, the number of cells was approximately 18 on day 1, and increased to 72 and 35 on the high- and low-collagen sides of the interface respectively. Similar trends were observed for the 0.2 % v/v (monomer A)−0.72 % v/v (monomer B) PAAM hydrogel, thereby, indicating that cellular migration was influenced by the chemical gradient. These results suggest that the chemical stimuli may have played a more significant role in directing the migration of fibroblast cells.

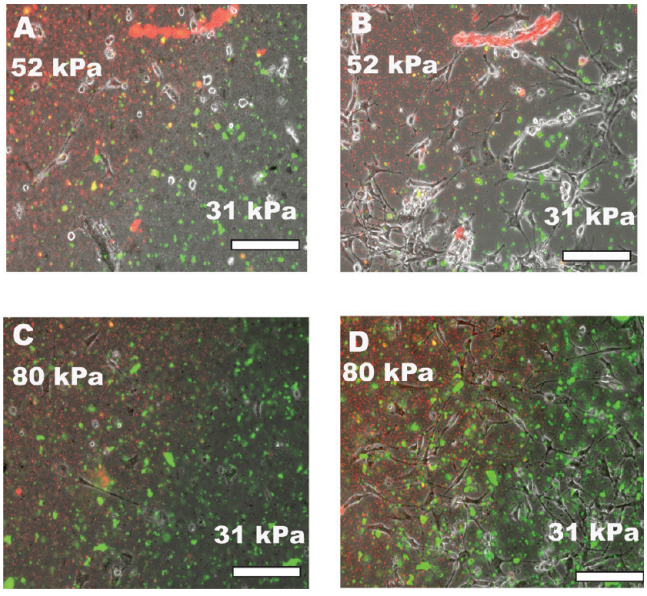

FIGURE 5. Accumulation of growth-arrested fibroblasts on the high collagen−low Young's modulus end of the interfacial region. (A) Day 1 and (B) day 5 for 0.2% v/v (monomer A)−0.56% v/v (monomer B) hydrogel; (C) day 1 and (D) day 5 for 0.2% v/v (monomer A)−0.72% v/v (monomer B) hydrogel. Scale bar = 100 μm.

DISCUSSION AND CONCLUSIONS

Cell motility is directed and modulated by a wide range of signals that cells receive and process. Among them, chemical and mechanical stimuli have been shown to play significant roles in guiding the direction of locomotion, and in the accumulation of cells. Cell motility is a dynamic process wherein cells are constantly probing their environment, extending lamellipodia, and simultaneously making and breaking links with the underlying substrate (41). We report the motion of single cells on a novel PAAM hydrogel substrate that exhibited a gradient in chemical and mechanical properties. Individual cells were the focus of this investigation in order to obtain insight into cell−-substrate interactions because cell−cell communications may dominate in cellular aggregates. 3T3 fibroblasts adhered on a substrate with a dual chemical and mechanical gradient were presented with simultaneous chemical and mechanical cues and had to make a choice in the direction of locomotion. Among the cells that traversed the interfacial region, the primary direction of motion was toward the high collagen−low Young's modulus end. A significant number of cells that had adhered initially on the high collagen−low Young's modulus end did not move across the gradient, after exploring their surrounding environment. These trends prevailed in all three interfacial regions that were investigated, thereby suggesting that the direction of fibroblast migration was influenced by the chemical gradient. It is of interest to note that fibroblasts cultured on the 0.56 % v/v (monomer A)−0.72 % v/v (monomer B) PAAM surface exhibited the highest (and statistically significant) average velocity despite exhibiting similar collagen surface coverage as the other substrates. It is hypothesized that substrate stiffness may have played a role in enabling optimal cell adhesion and subsequent motility. In the future, studies will be conducted on imaging the cytoskeletal structure and the size and location of focal adhesions in cells located at different positions within the interfacial region. These investigations will enable the correlation of focal adhesions with cell velocity and displacement values. In the future, detailed measurements will be conducted to determine the porosity of the interfacial region, because this

physical feature could potentially play a role in modulating cellular locomotion.

The elastic moduli of the PAAM substrates in this study were chosen carefully to match the values reported for various tissues and organs in vivo. For example, the Young's modulus for skin has been shown to vary between 14 kPa and 60 kPa based upon the underlying muscular contractions (42). The elastic modulus of cartilage has been observed to be in the 20 kPa to 30 kPa range (43) and the values for the elastic modulus of the liver ranges between 20 and 60 kPa (44, 45). Therefore, these studies could provide insights into the locomotion of cells within different tissues in the body. Furthermore, PAAM hydrogel substrates with a dual chemical-mechanical gradient, could serve as models to gain insight into the migratory behavior within tissues by incorporating tissue-specific cells and adhesive ligands. For applications in wound healing, the modulus of the substrates can be tuned to match scar tissue and these model systems can be used to glean information on the directed migration of cells toward soft scar tissue in wound healing applications. The novel opposing chemical and mechanical gradients reported here could provide a sound basis for the rational design of biomaterials for applications in tissue engineering and wound healing.

Understanding how a cell reacts when confronted with simultaneous and potentially conflicting cues is a fundamental question that has profound implications in multiple areas of biology and bioengineering. For example, tissue engineered devices and implants have to take into consideration the behavior of cells at the interfaces of tissues that exhibit vastly different properties. During tissue morphogenesis and organogenesis, cells migrate in response to a complex cocktail of signals. The abilities to match substrate rigidity to values found in vivo, link virtually any cell-adhesive ligand, and culture tissue-specific cells make our approach a general purpose methodology to probe migration in a wide range of tissues.

Acknowledgment. Parts of this work were carried out using instruments in the Nanoscale Characterization and Fabrication Laboratory, a Virginia Polytechnic Institute and State University facility operated by the Institute for Critical Technology and Applied Science.

REFERENCES AND NOTES

(1) Jacinto, A.; Martinez-Aria, A.; Martin, P. *Nat. Cell Biol.* **2001**, *3* (5), 117.
(2) Erickson, C. A.; Nuccitelli, R. *J. Cell Biol.* **1984**, *98* (1), 296.
(3) Thiery, J. P.; Duband, J. L.; Tucker, G. C. *Annu. Rev. Cell Biol.* **1985**, *1*, 91.
(4) Hendey, B.; Maxfield, F. R. *Blood* **1993**, *19* (1), 143.
(5) Maxfield, F. R. *Trends Cell Biol.* **1993**, *3* (11), 386.
(6) Cattaruzza, S.; Perris, R. *Matrix Biol.* **2005**, *24* (6), 400.
(7) Lauffenburger, D. A.; Wells, A. *Biophys. J.* **2003**, *84*, 3499.
(8) Liu, S.; Kapoor, M.; Leask, A. *Am. J. Pathol.* **2009**, *174* (5), 1847.
(9) Schmidt, C. E.; Horwitz, A. F.; Lauffenburger, D. A.; Sheetz, M. P. *J. Cell Biol.* **1993**, *123*, 977.
(10) Abramovitch, R.; Neeman, M.; Reich, R.; Stein, I.; Keshet, E.; Abraham, J.; Solomon, A.; Marikovsky, M. *FEBS Lett.* **1998**, *425* (3), 441.
(11) Seo, Y. K.; Yoon, H. H.; Song, K. Y.; Kwon, S. Y.; Lee, H. S.; Park, Y. S.; Park, J. K. *J. Orthop. Res.* **2009**, *27* (4), 495.
(12) Murray, M. M.; Spector, M. *Biomaterials* **2001**, *22* (17), 2393.
(13) Reinhart-King, C. A. *Methods Enzymol.* **2008**, *443*, 45.
(14) Sarvestani, A. S.; Jabbari, E. *Biotechnol. Bioeng.* **2009**, *103* (2), 424.
(15) Liu, J. C.; Tirrell, D. A. *Biomacromolecules* **2008**, *9* (11), 2984.
(16) Engler, A.; Bacakova, L.; Newman, C.; Hategan, A.; Griffin, M.; Discher, D. *Biophys. J.* **2004**, *86*, 617.
(17) Maheshwari, G.; Brown, G.; Lauffenburger, D. A.; Wells, A.; Griffith, L. G. *J. Cell Sci.* **2000**, *113*, 1677.
(18) Koo, L. Y.; Irvine, D. J.; Mayes, A. M.; Lauffenburger, D. A.; Griffith, L. G. *J. Cell Sci.* **2002**, *115*, 1423.
(19) Kim, S. V.; Mehal, W. Z.; Dong, X.; Heinrich, V.; Pypaert, M.; Mellman, I.; Dembo, M.; Mooseker, M. S.; Wu, D.; Flavell, R. A. *Science* **2006**, *314* (5796), 136.
(20) Reinhart-King, C. A.; Dembo, M.; Hammer, D. A. *Biophys. J.* **2008**, *95* (12), 6044.
(21) Discher, D. E.; Janmey, P.; Wang, Y. L. *Science* **2005**, *310* (5751), 1139.
(22) Lo, C. M.; Wang, H. B.; Dembo, M.; Wang, Y. L. *Biophys. J.* **2000**, *79* (1), 144.
(23) Wang, H. B.; Dembo, M.; Wang, Y. L. *Am. J. Physiol. Cell Physiol.* **2000**, *279* (5), C1345.
(24) Wang, H. B.; Dembo, M.; Hanks, S. K.; Wang, Y. L. *Proc. Natl. Acad. Sci. U. S. A.* **2001**, *98* (20), 11295.
(25) Munevar, S.; Wang, Y. L.; Dembo, M. *Biophys. J.* **2001**, *80* (4), 1744.
(26) Rajagopalan, P.; Marganski, W. A.; Brown, X. Q.; Wong, J. Y. *Biophys. J.* **2004**, *87* (4), 2818.
(27) Wong, J. Y.; Velasco, A.; Rajagopalan, P.; Pham, Q. *Langmuir* **2003**, *19*, 1908.
(28) Gray, D. S.; Tien, J.; Chen, C. *J. Biomed. Mater. Res.* **2003**, *66A*, 605.
(29) Ingber, D. E. *Int. J. Dev. Biol.* **2006**, *50*, 255.
(30) Engler, A. J.; Sen, S.; Sweeney, H. L.; Discher, D. E. *Cell,* **2006**, *126* (4), 677.
(31) Saranak, J.; Foster, K. W. *Nature* **1997**, *387* (6632), 465.
(32) Curtze, S.; Dembo, M.; Miron, M.; Jones, D. B. *J. Cell Sci.* **2004**, *117* (Pt 13), 2721.
(33) Guo, W. H.; Frey, M. T.; Burnham, N. A.; Wang, Y. L. *Biophys. J.* **2006**, *90* (6), 2213.
(34) Frey, M. T.; Tsai, I. Y.; Russell, T. P.; Hanks, S. K.; Wang, Y. L. *Biophys. J.* **2006**, *90* (10), 3774.
(35) Hadjipanayi, E.; Mudera, V.; Brown, R. A. *Cell Motil. Cytoskeleton* **2009**, *66* (3), 121.
(36) Grinnell, F.; Rocha, L. B.; Iucu, C.; Rhee, S.; Jiang, H. *Exp. Cell Res.* **2006**, *312* (1), 86.
(37) Shreiber, D. I.; Barocas, V. H.; Tranquillo, R. T. *Biophys. J.* **2003**, *84* (6), 4102.
(38) Beningo, K. A.; Lo, C. M.; Wang, Y. L. *Methods Cell Biol.* **2002**, *69*, 325.
(39) Domke, J; Radmacher, M. *Langmuir* **1998**, *14*, 3320–25.
(40) Frey, M. T.; Engler, A.; Discher, D. E.; Lee, J.; Wang, Y. L. *Methods Cell Biol.* **2007**, *83*, 48.
(41) DiMilla, P. A.; Stone, J. A.; Quinn, J. A.; Albelda, S. M.; Lauffenburger, D. *J. Cell Biol.* **1993**, *122* (3), 729.
(42) Zheng, Y. P.; Mak, A. F. T. In *Proceedings of the 19th IEEE/EMBS International Conference*; IEEE: Piscataway, NJ, 1997; p 2246.
(43) Stolz, M.; Raiteri, R.; Daniels, A. U.; Van Landingham, M. R.; Baschong, W.; Aebi, U. *Biophys. J.* **2004**, *86*, 3269.
(44) Nava, A.; Mazza, E.; Furrer, M.; Villiger, P.; Reinhart, W. H. *Med. Image Anal.* **2008**, *12* (2), 203.
(45) Sandrin, L.; Fourquet, B.; Hasquenoph, J. M.; Yon, S.; Fournier, C.; Mal, F.; Christidis, C.; Ziol, M.; Poulet, B.; Kazemi, F.; Beaugrand, M.; Palau, R. *Ultrasound Med. Biol.* **2003**, *29* (12), 1705.

AM100346K